

Non-blinking and photostable upconverted luminescence from single lanthanide-doped nanocrystals

Shiwei Wu^{a,1}, Gang Han^{a,1}, Delia J. Milliron^a, Shaul Aloni^a, Virginia Altoe^a, Dmitri V. Talapin^b, Bruce E. Cohen^{a,2}, and P. James Schuck^{a,2}

^aThe Molecular Foundry, Lawrence Berkeley National Laboratory, Berkeley, CA 94720; and ^bDepartment of Chemistry, University of Chicago, Chicago, IL 60637

Communicated by A. Paul Alivisatos, E. O. Lawrence Berkeley National Laboratory, Berkeley, CA, May 1, 2009 (received for review September 15, 2008)

The development of probes for single-molecule imaging has dramatically facilitated the study of individual molecules in cells and other complex environments. Single-molecule probes ideally exhibit good brightness, uninterrupted emission, resistance to photobleaching, and minimal spectral overlap with cellular autofluorescence. However, most single-molecule probes are imperfect in several of these aspects, and none have been shown to possess all of these characteristics. Here we show that individual lanthanide-doped upconverting nanoparticles (UCNPs)—specifically, hexagonal phase NaYF₄ (β -NaYF₄) nanocrystals with multiple Yb³⁺ and Er³⁺ dopants—emit bright anti-Stokes visible upconverted luminescence with exceptional photostability when excited by a 980-nm continuous wave laser. Individual UCNPs exhibit no on/off emission behavior, or “blinking,” down to the millisecond timescale, and no loss of intensity following an hour of continuous excitation. Amphiphilic polymer coatings permit the transfer of hydrophobic UCNPs into water, resulting in individual water-soluble nanoparticles with undiminished photophysical characteristics. These UCNPs are endocytosed by cells and show strong upconverted luminescence, with no measurable anti-Stokes background autofluorescence, suggesting that UCNPs are ideally suited for single-molecule imaging experiments.

bio-imaging | fluorescence | nanoparticle | single molecule | phosphorescence

Lanthanide-doped nanocrystals have recently shown promise as imaging probes due to their ability to upconvert low-energy near-infrared (NIR) radiation into higher-energy visible luminescence (1, 2). Unlike Stokes-shifted luminescence from organic- and protein-based fluorophores (3), semiconductor quantum dots (4–6), fluorescent latex (7) and silica (8) nanobeads, carbon nanotubes (9, 10), or newly developed nanodiamonds (11), this anti-Stokes luminescence circumvents competition from autofluorescent background signals in biological systems. The NIR-to-visible upconversion is based on sequential energy transfers between lanthanide dopants or excited-state absorption involving their real metastable-excited states with lifetimes as long as several milliseconds, a process orders of magnitude more efficient than the 2-photon absorption process typically used in multiphoton microscopy (12). For example, the UCNPs described here are approximately 10⁵ times more efficient at upconversion than many commonly used 2-photon fluorescence (TPF) dyes, including rhodamine 6G and fluorescein (13). This increased efficiency permits use of a continuous wave (CW) laser to generate the upconverted luminescence, resulting in virtually zero 2-photon photoluminescence background from biomolecules, since powerful pulsed-laser excitation is generally required for generating measurable multiphoton absorption. Use of NIR excitation also minimizes the possible photodamage in biological systems and permits deeper tissue penetration and whole-animal imaging.

While single-molecule imaging has become increasingly routine in biology (14), no probes with ideal single-molecule properties have been described. Significant progress has been made in the synthesis (1, 2, 15–20) and certain applications of UCNPs (15, 21–26), but their optical characterization has been limited to ensemble-averaged measurements. We show here that individual UCNPs are bright enough to be imaged with a modest-power CW laser, they exhibit no blinking, are exceptionally photostable, and they display no spectral overlap with cellular autofluorescence. We also find that UCNPs may be rendered water-soluble by wrapping with low molecular weight amphiphilic polymers, resulting in well-dispersed aqueous nanoparticles with undiminished photophysical characteristics. Polymer-wrapped UCNPs are endocytosed by murine fibroblasts and show strong upconverted luminescence, with no measurable anti-Stokes background autofluorescence. These findings suggest that UCNPs are ideally suited for single-molecule imaging experiments.

Results and Discussion

The UCNPs in these experiments are hexagonal phase NaYF₄ (β -NaYF₄) nanocrystals doped with 20% Yb³⁺ and 2% Er³⁺ ions, a composition optimized for efficient upconversion (1, 2). Their upconverted luminescence is dictated by lanthanide dopants (12, 27); the Yb³⁺ ions act as sensitizers that absorb 980-nm NIR excitation light without any visible upconverted emission and the Er³⁺ ions act as activators that emit visible upconverted luminescence characteristic of their atomic transitions. Excitation into these states is obtained by sequential energy transfers from neighboring sensitizers in the UCNP or excited-state absorptions (12).

The β -NaYF₄:Yb³⁺/Er³⁺ nanocrystals were prepared by a 2-step reaction, modified from the procedure of Mai, et al. (2) (see *SI Text* for details). The resulting UCNPs are single crystallites of roughly spherical shape and are uniform in size (Fig. 1A–C). From a detailed particle-size analysis of 300 particles from several transmission mode-scanning electron microscope (TM-SEM) images, the average particle size was found to be 26.9 nm with a standard deviation of 1.7 nm (Fig. 1C). A colloidal dispersion (0.01 wt%) of the UCNPs in hexane appears transparent, because of the low concentration of Er³⁺ ions and their low extinction coefficient (27) in the visible regime (Yb³⁺

Author contributions: S.W., G.H., D.J.M., D.V.T., B.E.C., and P.J.S. designed research; S.W., G.H., S.A., and V.A. performed research; S.W. and G.H. analyzed data; and S.W., G.H., D.J.M., B.E.C., and P.J.S. wrote the paper.

The authors declare no conflict of interest.

Freely available online through the PNAS open access option.

¹S.W. and G.H. contributed equally to this work.

²To whom correspondence may be addressed. E-mail: becohen@lbl.gov or pjschuck@lbl.gov.

This article contains supporting information online at www.pnas.org/cgi/content/full/0904792106/DCSupplemental.

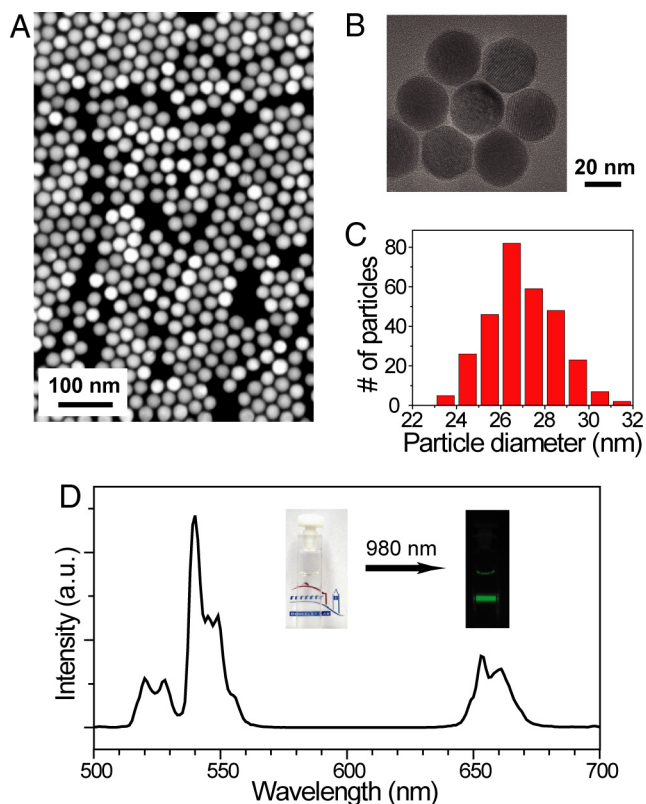


Fig. 1. Lanthanide-doped UCNPs ($\text{NaYF}_4:\text{Yb}^{3+}/\text{Er}^{3+}$) showing near-infrared to visible upconverted luminescence. (A and B) TM-SEM and TEM images of the UCNPs. (C) A histogram of particle sizes obtained from TM-SEM images of approximately 300 nanoparticles (average particle size = 26.9 ± 1.7 nm). (D) Upconverted luminescence spectrum of the UCNPs (0.01 wt%) diluted in hexane when excited by a 980-nm CW diode laser at power density of approximately 8 W/cm^2 . Upconverted visible emission bands are centered at 540 nm and 655 nm. (Inset) Photographs of the transparent solution without laser illumination and the upconverted visible luminescence under laser illumination.

has no electronic transitions in the visible), but irradiation with a 980-nm CW diode laser at power density of approximately 8 W/cm^2 produces visible light obvious to the naked eye (Fig. 1D, Inset). The upconverted luminescence spectrum of these UCNPs (Fig. 1D) exhibits 2 distinct Er^{3+} emission bands, in the green (515–560 nm) and red (640–670 nm) regions of the spectrum (1, 2). The 2 emission bands are the result of a multiphoton upconversion process (2), as suggested by power-dependent emission intensity at relatively low excitation power density (see Fig. S1).

To examine the optical properties of individual UCNPs, we dispersed a dilute sample of UCNPs on a silicon nitride membrane and spectroscopically imaged them in a sample-scanning confocal optical microscope while exciting with a tightly focused 980-nm CW laser. At each pixel, visible luminescence was either collected by a single photon avalanche photodiode (SPAD) or by a spectrograph equipped with a charge-coupled device (CCD) detector. An upconverted luminescent image of the sample (Fig. 2A) shows homogeneous and randomly distributed diffraction-limited spots on the membrane, while the background intensity reflects the dark counts of the SPAD. By collecting optical spectra from individual luminescent spots (Fig. 2B), we observe that the upconverted visible emission bands are centered at approximately 550 nm and 655 nm, characteristic of Er^{3+} atomic transitions. However, the intensity of the red emission band becomes stronger than that of the green emission band, in

contrast to the ensemble-averaged measurement at much lower laser power density (Fig. 1D), due to different upconversion pathways for the 2 colors (2) and the change of their upconversion efficiency at high laser power density used for single UCNPs (see Figs. S1 and S2).

The confocal optical characterization suggests that the upconverted luminescent spots may originate from single UCNPs. However, because the optical diffraction limit is about 20 times larger than the average particle size, there remains a possibility that individual spots may include more than one UCNP. To determine if each diffraction-limited spot arises from a single UCNP, we imaged the same region of the sample in a TM-SEM. A TM-SEM image (Fig. 2A, Inset) of an area corresponding to a constellation of UCNPs in the upper left corner of the confocal optical image shows five spots that have identical inter-particle distances in both images, and whose shape and size are consistent with those in Fig. 1C (see Fig. S3 and Table S1). Their identities are further confirmed by X-ray energy-dispersive spectroscopy (EDS) in a transmission electron microscope (TEM, Fig. 2C), carried out on over 20 individual UCNPs as well as nearby impurities (such as spot F, Fig. 2A, Inset). EDS analysis of the luminescent spots shows compositional uniformity, while irregular, non-luminescent spots are revealed to be low atomic weight contamination. All spots identified by TM-SEM and X-ray EDS as UCNPs appeared bright by confocal imaging, suggesting that there are no “dark” nanoparticles, in contrast to what has been found in commercial quantum dot preparations (28). Note that the TM-SEM and EDS analysis were carried out after all optical characterization to avoid perturbing the optical properties caused by high-energy electrons.

To determine the photostability of these UCNPs under conditions used for single-molecule microscopy, a single UCNP was kept under continuous 10 mW (equivalent to $\approx 5 \times 10^6 \text{ W/cm}^2$) 980-nm CW laser illumination for an extended time. All upconverted visible photons were collected and time-tagged with a time-correlated single-photon-counting (TCSPC) set-up, permitting multiple types of subsequent data analysis. No photobleaching or photodamage was observed after 1 h of continuous laser illumination (Fig. 3A). In particular, emission fluctuation and intermittency (i.e., blinking), commonly observed in single semiconductor quantum dots (29) and single fluorophores (30), were not observed. To further demonstrate the non-blinking behavior, the bin time for each data point in emission intensity was reduced to 1 ms (Fig. 3B). A histogram of emission intensity (Fig. 3C) follows a Poisson distribution, suggesting that the upconverted luminescence is shot noise limited and no other photon noise sources, such as blinking, are observed down to 1 ms (31). This observation differs from luminescence in a single nanocrystal doped with a single lanthanide ion, where blinking was observed and associated with the inherently long excited-state lifetime (up to several milliseconds) of lanthanide ions (32). In our experiment, each UCNP contains approximately 700 Er^{3+} ions and 7,000 Yb^{3+} ions based on the EDS analysis and average particle size, so that this non-blinking is due to the steady-state emissions from multiple ions in a single UCNP (32, 33). The absence of photobleaching and blinking significantly improves signal-to-noise and signal-to-background statistics, allowing one, for example, to precisely and quickly determine the center position of individual UCNPs with nanometer-scale accuracy (34), or to track cellular proteins for extended periods without uncertainties arising from intermittent loss of emission (35).

For UCNPs to be useful as bioimaging probes, they need to be water-soluble while retaining their photophysical properties (19, 24). Hydrophobic oleic acid-coated $\beta\text{-NaYF}_4:\text{Yb}^{3+}/\text{Er}^{3+}$ nanoparticles were rendered water-soluble by wrapping with low molecular weight ($\approx 3,000$ Da) amphiphilic polymers,

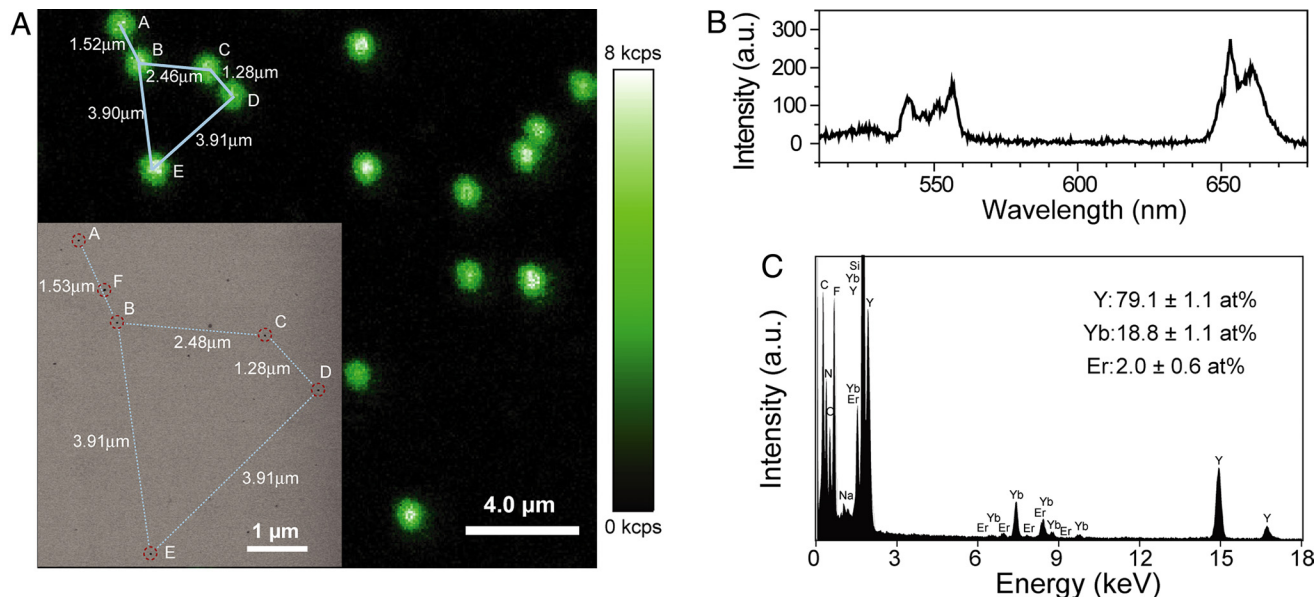


Fig. 2. Individual UCNPs on a silicon nitride membrane. (A) Confocal upconverted luminescent image of individual UCNPs. Laser power density is approximately 3×10^6 W/cm², and dwell time per pixel is 10 ms. The TM-SEM image (*inset*) taken at the upper left corner region of the optical image shows that the individual diffraction-limited luminescent spots are emitted from individual UCNPs. The 5 individual UCNPs are labeled as A–E; an impurity is labeled as F. (see Fig. S3 and Table S1, for their TM-SEM images and local chemical compositions.) (B) Upconverted luminescence spectrum of a single UCNP. (C) EDS of the UCNP labeled as C in A. From the EDS analysis of 20 individual UCNPs, the averaged ratios and their standard deviations of different elements (Y, Yb, and Er) are obtained and also noted in C.

resulting in well-dispersed aqueous UCNPs (see Fig. S4). These UCNPs exhibited diffraction-limited upconversion luminescent spots with similar intensities as hydrophobic UCNPs

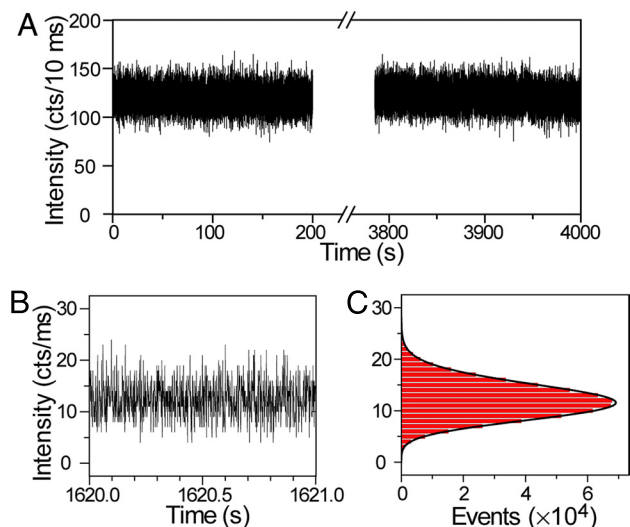


Fig. 3. Photostability and non-blinking behavior of a single UCNP. (A) The time trace of emission intensity from a single UCNP under continuous laser illumination for more than 1 h, suggesting the durable photostability of the UCNPs. The bin time for each data point is 10 ms. The laser power used on the sample is approximately 10 mW, corresponding to a power density of $\approx 5 \times 10^6$ W/cm². (B and C) The zoom-in time trace and histogram of emission intensity, showing no on/off behavior – non-blinking. Note that the bin time for each data point in (B and C) is reduced to 1 ms for higher time resolution. The histogram is fitted with a Poisson distribution function,

$$y(l) = A \frac{e^{-\lambda} \lambda^l}{l!},$$

where l is the emission intensity, A is the number of total events (6×10^5), and λ is the fitting parameter ($\lambda = 12.066 \pm 0.009$).

(Figs. 4A and S5). A histogram of emission intensity from over 200 luminescent spots (Fig. 4B) shows a dominant peak, suggesting that most are from single UCNPs. Aqueous UCNPs exhibit similar non-blinking behavior and resistance to bleaching as hydrophobic UCNPs (Fig. 4C and D). The hydrophobic UCNPs were also made water-soluble by exchange of surface oleic acid with citric acid (24), but citric acid coatings appear to adversely affect the emission intensity of the UCNPs (see Fig. S5).

To demonstrate the potential of UCNPs as probes for biological imaging, we incubated amphiphilic polymer-coated UCNPs with murine fibroblasts and allowed them to be endocytosed. Confocal images show strong upconverted luminescence is visible in cells with endocytosed UCNPs under 980-nm CW laser illumination (Figs. 5B), but cells without UCNPs show no measurable upconverted luminescence under identical imaging conditions (Figs. 5E). However, cells excited with 532-nm CW laser illumination did show significant cellular autofluorescence (Fig. 5F), indicating, as expected, Stokes-shifted background arising from endogenous compounds in the cell.

Conclusion

We have demonstrated that individual lanthanide-doped nanocrystals possess ideal properties for single-molecule imaging, including anti-Stokes upconverted visible luminescence, non-blinking emission, exceptional photostability, and noninvasive NIR excitation, which can minimize cell damage and scatter. Upconversion in these particles is highly efficient, needing excitation from only a CW laser source, in marked contrast to other multiphoton imaging techniques that require high peak powers from pulsed laser excitation. The characteristics of these nanoparticles suggest that they could serve as ideal single-molecule imaging probes for both *in vitro* and *in vivo* studies, particularly because of the absence of efficient upconverting compounds in the cell. Use of UCNPs may be extended to sensing, cellular targeting, energy transfer and other applications, through surface conjugation of organic or biological molecules, to create functionally diverse imaging probes.

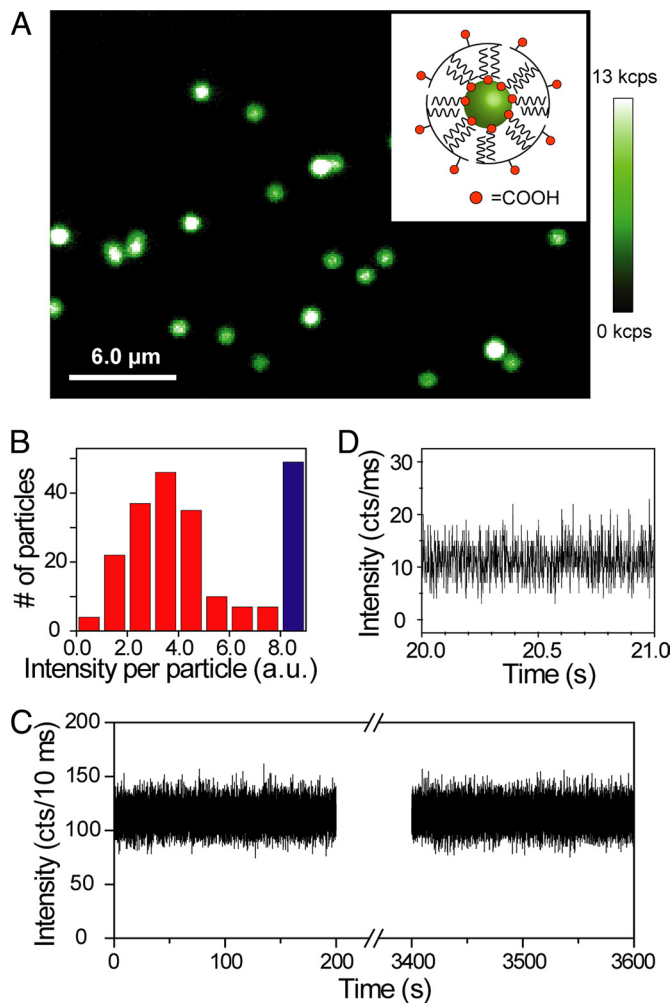


Fig. 4. Upconverted luminescence of individual water-soluble UCNPs. (A) Confocal upconverted luminescent image of individual amphiphilic polymer-coated UCNPs (schematically shown in the *Inset*) sparsely dispersed on a clean coverglass. The laser power is approximately 10 mW, equivalent to approximately 5×10^6 W/cm². Some of the bright luminescent spots represent multiple UCNPs within the diffraction limited area, generating saturated “white” spots in the image. (B) A histogram of integrated emission intensity from over 200 upconverted luminescent spots, suggesting that most of the luminescent spots are from single polymer-coated UCNPs. The data were analyzed from confocal upconverted luminescent images over a $75 \times 75 \mu\text{m}$ area, and the number of saturated “white” spots was shown in the histogram as a blue bar. Such single water-soluble UCNPs also exhibit exceptional photostability (C) and non-blinking behavior (D).

Materials and Methods

Sample Preparation and Electron Microscopic Characterizations. A sample of oleic acid-coated UCNPs for single-particle characterization was prepared by drop casting a dilute solution of UCNPs in hexane on a 20-nm thick silicon nitride membrane window (4107SN-BA, SPI Supplies), which allowed both optical and electron microscopic characterization. The window size of $100 \mu\text{m}$ permitted us to inspect the same region of interest in a SEM at 30 kV (FESEM-Ultra 55, Zeiss) and in a TEM at 200 kV (FETEM-2100F, Jeol) equipped with an energy dispersive X-ray

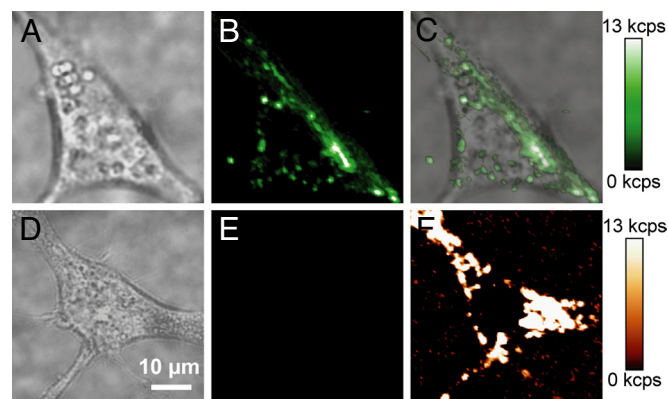


Fig. 5. Live-cell imaging of UCNPs in NIH 3T3 murine fibroblasts. (A) Brightfield image of a cell with endocytosed UCNPs, (B) upconverted luminescence following 980-nm excitation, and (C) overlay. (D) Brightfield image of a cell without UCNPs, (E) upconverted luminescence following 980-nm excitation, and (F) cellular autofluorescence following 532-nm excitation. All confocal images are shown on the same intensity scale. (Scale bar, $10 \mu\text{m}$.)

spectrometer (INCAEnergyTEM250, Oxford), after optical characterization. The region of interest was mapped using a transmission mode in the SEM (TM-SEM) as well as the TEM. The morphology, structure and composition of individual nanoparticles were obtained by HR-TEM and EDS. The samples of individual amphiphilic polymer-coated UCNPs and citric acid-coated UCNPs were prepared on a separate polyD-Lysine pretreated coverglass by drop casting.

Optical Characterization. Upconverted luminescence of individual UCNPs was characterized in a modified sample-scanning confocal optical microscope (TE-2000U, Nikon). A 980-nm single-mode CW diode laser (L980P300, Thorlabs) was tightly focused on the sample through a 0.95 NA 100X air objective (Plan Apo, Nikon). The sample was raster scanned by a piezo-actuated three-dimensional nanopositioning stage (Nano-PDQ375, Madcity). At each pixel, the upconverted visible luminescence was collected through the same objective, and passed through a dichroic beamsplitter (750DCSPXR, Chroma) and 2 short-pass filters (700SP-2P and 750SP-2P, Chroma), while the 980-nm excitation light was completely filtered out. After passing through a confocal pinhole ($150 \mu\text{m}$), the upconverted luminescence was either detected by a SPAD (SPCM-AQR-15, Perkin-Elmer) or by a spectrograph (SP-2356, Acton) equipped with a CCD detector (iXon, Andor). The upconverted photons detected by the SPAD can also be recorded and time-tagged with a TCSPC (PicoHarp 300, PicoQuant).

Cell Culture and Imaging. NIH 3T3 mouse embryonic fibroblasts (ATCC) were grown to 70% confluence on polyD-lysine coated glass-bottom dishes (MatTek) in modified high-glucose DMEM with 10% FBS. Cells were incubated for 3 h with 10 pM amphiphilic polymer-coated UCNPs in DMEM with FBS, humidified at 37°C under 5% CO_2 . Cells were washed 3 times with PBS and then resuspended in DMEM for imaging. Images were acquired with a 1.4 NA 100X oil objective (Plan Apo, Nikon) on the same confocal optical microscope as described above. Upconverted luminescence was excited with a 980-nm CW laser at a power of approximately 10 mW and cellular autofluorescence with a 532-nm CW laser at a power of approximately 85 μW . A Z532RDC dichroic beamsplitter (Chroma) and 3RD540LP emission filter (Omega Optical) were used for autofluorescent images, and optics for upconverted images were the same as described above.

ACKNOWLEDGMENTS. We thank Miquel Salmeron for support and for constructive comments on the manuscript. Work at the Molecular Foundry was supported by the Director, Office of Science, Office of Basic Energy Sciences, Division of Materials Sciences and Engineering, of the U.S. Department of Energy under Contract No. DE-AC02-05CH11231.

- Heer S, Kompe K, Gudel HU, Haase M (2004) Highly efficient multicolour upconversion emission in transparent colloids of lanthanide-doped NaYF₄ nanocrystals. *Adv Mater* 16:2102–2105.
- Mai H-X, Zhang Y-W, Sun L-D, Yan C-H (2007) Highly efficient multicolor up-conversion emissions and their mechanisms of monodisperse NaYF₄:Yb,Er core and core/shell-structured nanocrystals. *J Phys Chem C* 111:13721–13729.
- Weiss S (1999) Fluorescence spectroscopy of single biomolecules. *Science* 283:1676–1683.

- Alivisatos AP, Gu W, Larabell C (2005) Quantum dots as cellular probes. *Annu Rev Biomed Eng* 7:55–76.
- Medintz IL, Uyeda HT, Goldman ER, Mattoussi H (2005) Quantum dot bioconjugates for imaging, labeling, and sensing. *Nat Mater* 4:435–446.
- Michalet X, et al. (2005) Quantum dots for live cells, in vivo imaging, and diagnostics. *Science* 307:538–544.
- Taylor JR, Fang MM, Nie S (2000) Probing specific sequences on single DNA molecules with bioconjugated fluorescent nanoparticles. *Anal Chem* 72:1979–1986.

